Available online at www.sciencedirect.com
ScienceDirect
Journal of Sound and Vibration 312 (2008) 630–643
JOURNAL OF SOUND AND VIBRATION
www.elsevier.com/locate/jsvi

The anti-oscillator model parameters linked to the apparent mass frequency response function

E. Jacquelin[a,b,c,*], J.-P. Lainé[a,d,e], A. Bennani[a,b,c], M. Massenzio[a,b,c]

[a]*Université de Lyon, Lyon, F-69003, France*
[b]*Université Lyon 1, IUT B, LBMC, Villeurbanne, F-69627, France*
[c]*INRETS, UMR-T 9406, Bron, F-69675, France*
[d]*Ecole Centrale de Lyon, LTDS, Ecully, F-69134, France*
[e]*CNRS, UMR 5513, Ecully, F-69134, France*

Received 25 July 2007; received in revised form 29 October 2007; accepted 5 November 2007
Available online 20 February 2008

Abstract

A finite element model of a structure provides a fine knowledge of the response but such a model may lead to a loss of a global comprehension of the structural behaviour. That is why the anti-oscillator model (AO model), that may be derived from a finite element model, was developed. The mass and stiffness matrices are required but they often can not be retrieved easily in the commercial softwares. This paper shows how to overcome this problem and finally how to avoid a numerical model of a structure to derive the AO characteristics.

In fact, it is shown that the AO characteristics and the apparent mass frequency response function (FRF) are closely tied. Indeed, the AO mass are the residue of the partial fraction decomposition of this FRF, while AO frequencies are the poles. Consequently, the AO characteristics can easily be derived from an experiment which allow the determination of the apparent mass FRF.

1. Introduction

The most commonly used technique to model a structure is the finite element method [1]. This method is very general and may be used to solve different kind of problems such as static problems, modal analysis and stability analysis. Nevertheless, such a modelling may lead to a lot of degrees-of-freedom (dof) whereas, sometimes, few dof are sufficient. This may lead to a non-efficient model. A new approach has been proposed recently to transform a finite element model to an efficient model based on the anti-oscillators (AOs) [2].

The AOs are linked to the antiresonant frequencies [3] and to the shapes associated with these frequencies. It was not new to use such an information to update a model [4–6] and then to improve the knowledge of a system; the antiresonant frequencies have been used for crack detections in beams as well [7]. Nevertheless, these studies did not use the antiresonances to directly model a structure until the work reported by Jacquelin

*Corresponding author at: Université de Lyon, Université Claude Bernard Lyon I - INRETS, LBMC, UMR-T 9406, IUT B, 17 rue de France, 69627 Villeurbanne, France. Tel.: +33 472692132; fax: +33 472692120.
E-mail address: eric.jacquelin@univ-lyon1.fr (E. Jacquelin).

0022-460X/$ - see front matter © 2007 Elsevier Ltd. All rights reserved.
doi:10.1016/j.jsv.2007.11.007

et al. [2] which introduced the notion of AOs. An application of the AO model had been done by Pashah et al. in Ref. [8] to understand and forecast the behaviour of impacted structures.

Nevertheless, in Ref. [2] a first model of the structure is required to identify the AO characteristics. So, this first model must be updated carefully to derive a good AO formulation. This paper shows how to derive the parameters of this new model experimentally by measuring an apparent mass frequency response function (FRF) so that the first model is avoided.

In the following, the AOs are presented first. Particularly the AO characteristics are defined from the mass M and stiffness K operators (or matrices) which are supposed to be known. The determination of the AO parameters from an FRF without any model is then undertaken. Finally, some examples are given to show the efficiency and the simplicity of the method.

2. The anti-oscillator model

The AO model is briefly described in this section where no proof is given; more information may be found in Ref. [2].

When an action effect acts on a structure at a point P in a given direction, the response changes if the load direction or the point location change. Consequently, the "best" model of a structure depends on the location and the direction of the action effect. The AO formulation was proposed to consider that remark. Then the AO formulation is attached to a point P and to a given direction, i.e. to a given dof i_0 of the studied structure. This description is particularly appropriate for impact problems, when the impact location and direction were known [8]. Nevertheless, this approach is more general and may be used with all kinds of loads and, above all, it explains how the structure globally behaves when excited along a specific dof.

2.1. Static, constraint and residual modes

2.1.1. Static mode

The static mode ϕ_{st} is the shape of the structure when a load F_{st} is applied, such that $\phi_{\mathrm{st}\,i_0}$ is equal to unity (see Fig. 1). Note that for the statically indeterminate structures ϕ_{st} is a rigid body mode.

2.1.2. Constraint modes

The constraint modes ϕ_i, $\omega_{\mathrm{AR}\,i}$ are the eigenmodes of the structure submitted to an extra boundary condition (see Fig. 1):

$$\phi_{ii_0} = 0. \tag{1}$$

Then the eigenfrequencies $\omega_{\mathrm{AR}\,i}$ are the antiresonant frequencies of the structure [3] which depend on i_0.

2.1.3. Residual mode

The residual mode ϕ_0 is spanned by the static mode and by the constraint vectors and is such that the residual mode is orthogonal to each constraint vector with respect to the mass operator. Then ϕ_0 verifies:

$$\phi_0 = \phi_{\mathrm{st}} - \sum_{i=1}^{+\infty} c_i \phi_i. \tag{2}$$

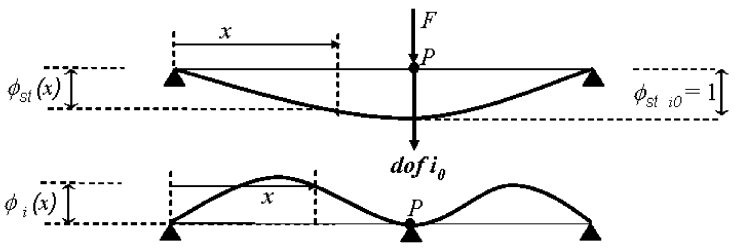

Fig. 1. Static and constraint modes of a beam.

The coefficients c_i may easily be determined, owing to the orthogonal property between ϕ_0 and the constraint modes $\{\phi_i\}_{i=1..+\infty}$.

2.1.4. Kinematic description

The static and the residual modes were introduced for two main reasons:

- when a structure is loaded by a quasi-static excitation in the direction of the dof i_0, the model must allow for the static stiffness: the AO model allows the determination of such a static stiffness thanks to the static mode;
- when a structure is loaded by an excitation, which is dynamic in nature, in the direction of the dof i_0, the inertia effects act against the action effect to prevent the motion of the dof i_0; so, at least during the very beginning of the impact, the inertia effects act as an extra boundary condition. Therefore, the displacement should be well described by the constraint modes.

The idea was then to expand the solution in terms of the static and the constraint modes. Unfortunately, the static mode cannot be orthogonal to the constraint modes. So, the displacement X was expanded in terms of the residual and the constraint modes, i.e. in terms of a sum of orthogonal functions with respect to the mass operator:

$$X(t) = \sum_{i=0}^{+\infty} q_i(t)\phi_i. \tag{3}$$

The discretization was achieved by truncating the expansion (3) at the rank N:

$$X(t) \simeq X^d(t) = \sum_{i=0}^{N} q_i(t)\phi_i. \tag{4}$$

2.2. The anti-oscillators

The discretized displacement (4) may also be written as

$$\begin{aligned} X^d(t) &= q_0(t)\phi_0 + \sum_{i=1}^{N} q_i(t)\phi_i \\ &= \lambda_0(t)\psi_0 + \sum_{i=1}^{N} (\lambda_i(t) - \lambda_0(t))\psi_i, \end{aligned} \tag{5}$$

where

$$\begin{aligned} &\lambda_0(t) = q_0(t), \quad \psi_0 = \phi_{\mathrm{st}}, \\ &\lambda_i(t) = \frac{q_i(t)}{c_i}, \quad \psi_i = c_i\phi_i. \end{aligned} \tag{6}$$

Actually, this change of variable was very interesting because it led to a representation of any structure with N single-dof systems $(m_i,\ k_i)_{i=1..N}$ lying on a single-dof system $(m_0,\ k_0)$. The degrees of freedom were then the $N+1$ parameters $\{\lambda_i\}_{i=0..N}$. The single-dof systems $(m_i,\ k_i)_{i=1..N}$ were referred to be "anti-oscillators" [2]. In fact Eq. (5) indicates that λ_0 is equal to the dof of interest, i_0 due to the definition of the ψ_i functions.

In Ref. [2] it was shown that the masses represented in Fig. 2 may be expressed as:

- *for* $i>0$:

$$m_i = M(\phi_i, \phi_i)c_i^2 = \frac{M(\phi_{\mathrm{st}}, \phi_i)^2}{M(\phi_i, \phi_i)}, \tag{7}$$

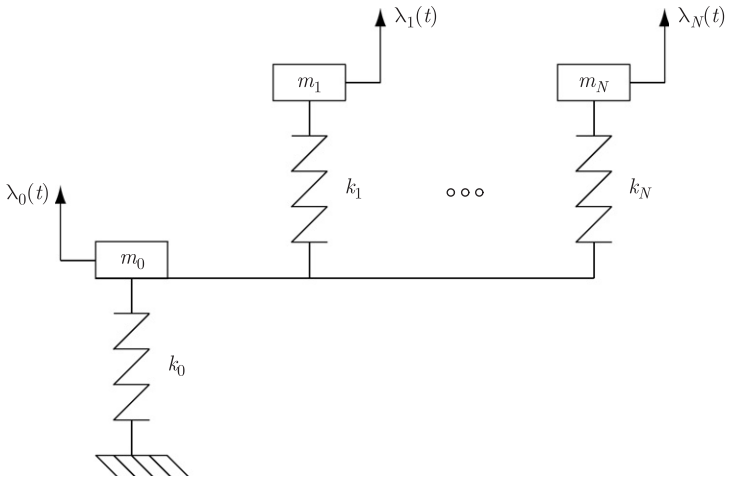

Fig. 2. Model of a structure impacted by another structure.

- *for* $i = 0$:

$$m_0 = M(\phi_{\mathrm{st}}, \phi_{\mathrm{st}}) - \sum_{i=1}^{N} \frac{M(\phi_{\mathrm{st}}, \phi_i)^2}{M(\phi_i, \phi_i)} = m_{\mathrm{st}} - \sum_{i=1}^{N} m_i, \tag{8}$$

where M is the mass operator (i.e. the mass matrix for discretized system).

Likewise, the stiffnesses $\{k_i\}_{i=0\cdots N}$ can be identified:

- $i = 0$:

$$k_0 = K(\psi_0, \psi_0) = K(\phi_{\mathrm{st}}, \phi_{\mathrm{st}}). \tag{9}$$

  Then,
  - for statically determinate structures, k_0 is the static stiffness.
  - for statically indeterminate structures (i.e. ϕ_{st} is a rigid body eigenshape), $k_0 = 0$.
- $i = 1 \cdots N$:

$$k_i = \omega_{\mathrm{AR}\,i}^2 m_i. \tag{10}$$

In the following the AOs will be sorted on the basis of their frequency so that the frequency increases with the ascending number of AOs.

3. The AO parameters and the apparent mass FRF

Ewins FRF [9] defined the apparent mass FRF as the inverse inertance. The point apparent mass FRF associated with the dof λ_0 will be used in that paper.

Considering a harmonic force applied in the direction of the displacement λ_0 which is the i_0^{th} dof:

$$f_h(t) = F_h \mathrm{e}^{\mathrm{j}\omega t}. \tag{11}$$

Each component $\lambda_i(t)$ of the displacement given by Eq. (5) is harmonic as well and may be written as following:

$$\forall i \geqslant 0, \quad \lambda_i(t) = \Lambda_i \mathrm{e}^{\mathrm{j}\omega t}. \tag{12}$$

By considering Fig. 2, the dof verify the following equations:

- $i>0$:

$$m_i\ddot{\lambda}_i(t)+k_i(\lambda_i(t)-\lambda_0(t))=0. \tag{13}$$

Relation (11) leads to:

$$-\omega^2 m_i \Lambda_i + k_i(\Lambda_i-\Lambda_0)=0. \tag{14}$$

As $\omega^2_{\mathrm{AR}\,i}=k_i/m_i$, this equation may be rewritten as

$$\Lambda_i=\frac{\Lambda_0}{1-(\omega^2/\omega^2_{\mathrm{AR}\,i})}. \tag{15}$$

- $i=0$:

$$m_0\ddot{\lambda}_0(t)+k_0\lambda_0(t)-\sum_{l=1}^{N}k_i(\lambda_i(t)-\lambda_0(t))=f_h(t). \tag{16}$$

Eqs. (11) and (15) lead to:

$$-\omega^2 m_0\Lambda_0+k_0\Lambda_0-\sum_{l=1}^{N}k_i\left(\frac{1}{1-(\omega^2/\omega^2_{\mathrm{AR}\,i})}-1\right)\Lambda_0=F_h. \tag{17}$$

Then the point dynamic stiffness FRF is

$$\frac{F_h}{\Lambda_0}=-\omega^2 m_0+k_0+\sum_{l=1}^{N}\frac{-\omega^2 m_i}{1-(\omega^2/\omega^2_{\mathrm{AR}\,i})} \tag{18}$$

The point apparent mass FRF M_{app}, which is the requested FRF for this study, may be deduced:

$$M_{\mathrm{app}}=\frac{F_h}{\Gamma_0}=\frac{F_h}{-\omega^2\Lambda_0}=m_0-\frac{k_0}{\omega^2}+\sum_{l=1}^{N}\frac{m_i}{1-(\omega^2/\omega^2_{\mathrm{AR}\,i})} \tag{19}$$

where the acceleration is $\ddot{\lambda}_0(t)=-\omega^2\Lambda_0 e^{j\omega t}=\Gamma_0 e^{j\omega t}$.

This result shows that it is possible to determine the AO parameters from experiments:

- k_0 is determined from a static test with a static force applied at P in the direction of the dof i_0 (see Fig. 1); alternatively, k_0 is the amount of the dynamic stiffness FRF when ω is equal to zero.
- m_{st} is determined from the M_{app} FRF:

$$m_{\mathrm{st}}=m_0+\sum_{l=1}^{N}m_i=M_{\mathrm{app}}(\omega=0)+\frac{k_0}{\omega^2}. \tag{20}$$

Note that for the indeterminate structures, $k_0=0$ and the "static" mass is the rigid body mass:

$$m_{\mathrm{st}}=m_0+\sum_{l=1}^{N}m_i=M_{\mathrm{app}}(\omega=0). \tag{21}$$

- The antiresonant circular frequency $\omega_{\mathrm{AR}\,i}$ are the poles of the M_{app} FRF;
- m_i is identified as the residue associated with the pole $\omega_{\mathrm{AR}\,i}$ of the M_{app} FRF;
- m_0 is then deduced as

$$m_0=m_{\mathrm{st}}-\sum_{i=1}^{N}m_i.$$

This method will be applied in the following to derive the AO parameters from either numerical or experimental FRF.

4. Free–free bar: numerical experiment

The studied system was an indeterminate structure in which the bar was made of steel and of circular cross section. The material and geometrical properties of the bar are given in Table 1.

4.1. Anti-oscillator characteristics from an FE model

The AO parameters from a finite element model were determined firstly from the mass and stiffness matrices as explained in Ref. [2]. The bar was discretized in n_e 2-node elements, with one dof per node and linear interpolation for the displacement. n was the total number of dof. The AO parameters were associated with the i_0^{th} dof. Then, a reduced mass matrix $\mathbf{M}^{\text{red}}$ and a reduced stiffness matrix $\mathbf{K}^{\text{red}}$ can be derived from the mass matrix $\mathbf{M}$ and the stiffness matrix $\mathbf{K}$ by replacing the i_0^{th} row and the i_0^{th} column by a row and a column filled with zeros in each matrix. The constraint modes $\{\mathbf{\Phi}_i, \omega_{\text{AR}\ i}\}_{i=1..n}$ are the modes obtained from the reduced mass and stiffness matrices. The static mode $\mathbf{\Phi}_{\text{st}}$ is actually the rigid-body mode of the structure. Then the AO parameters are evaluated as following:

$$c_i = \frac{\mathbf{\Phi}_\mathbf{i}^t \mathbf{M} \mathbf{\Phi}_{\text{st}}}{\mathbf{\Phi}_\mathbf{i}^t \mathbf{M} \mathbf{\Phi}_\mathbf{i}} \tag{22}$$

$$\mathbf{\Phi_0} = \mathbf{\Phi}_{\text{st}} - \sum_{i=1}^{n-1} c_i \mathbf{\Phi}_\mathbf{i} \tag{23}$$

$$m_{\text{st}} = \mathbf{\Phi}_{\text{st}}^t \mathbf{M} \mathbf{\Phi}_{\text{st}} \tag{24}$$

$$m_i = c_i^2 \mathbf{\Phi}_\mathbf{i}^t \mathbf{M}^{\text{red}} \mathbf{\Phi}_\mathbf{i} = \frac{(\mathbf{\Phi}_\mathbf{i}^t \mathbf{M}^{\text{red}} \mathbf{\Phi}_{\text{st}})^2}{\mathbf{\Phi}_\mathbf{i}^t \mathbf{M}^{\text{red}} \mathbf{\Phi}_\mathbf{i}} \tag{25}$$

$$k_0 = \mathbf{\Phi}_{\text{st}}^t \mathbf{K} \mathbf{\Phi}_{\text{st}} \tag{26}$$

$$k_i = \omega_{\text{AR}\ i}^2 m_i \tag{27}$$

The characteristics of the five first AOs were listed in Table 2. In fact, the "static" mass was the bar mass $m_{\text{st}} = 1.73\,\text{kg}$ and the stiffness k_0 was zero (statically undetermined structure).

Table 1
Properties of the bar

E (GPa)	ρ (kg m^{-3})	d (mm)	L (mm)
210	7800	30	313

Table 2
Characteristics of the AO bar model

AO number	1	2	3	4	5
Mass m_i (g)	1398.8	155.4	56.0	28.5	17.3
Frequency f_{AR} (kHz)	4.14	12.44	20.74	29.07	37.43

4.2. Anti-oscillator characteristics from the mass FRF

The FRF was built from the eigenmodes $\{\mathbf{\Psi}_i, \Omega_i\}_{i=1..n}$ derived from the mass and stiffness matrices. In the following, the eigenvectors were normalized with respect to the mass matrix. First the following FRF was evaluated:

$$H = \frac{\Lambda_O}{F_h} = \sum_{i=1}^{n} \frac{\mathbf{\Psi}_{ii_0}^2}{\Omega_i^2 - \omega^2 + 2\xi\omega\Omega_i}, \tag{28}$$

where ξ is the dimensionless damping ratio. Ψ_{ii_0} indicates that H is a point FRF associated with the i_0 dof. H is a sum of rational functions then H may be written as

$$H = \frac{N_H(\omega)}{D_H(\omega)}, \tag{29}$$

where N_H and D_H are two polynomials.

The apparent mass M_{app} is the inverse of H divided by $(-\omega^2)$:

$$M_{\text{app}}(\omega) = \frac{D_H(\omega)}{-\omega^2 N_H(\omega)}. \tag{30}$$

So M_{app} is a rational function: the numerator and the denominator may be identified from an experimental curve. A partial fraction decomposition of the apparent mass M_{app} (30) is then achieved. Eq. (19) shows that the residue associated with a pole, which is the ith antiresonant frequency, is the mass m_i.

4.3. Results

The apparent mass FRF was sketched in Fig. 3 for a damping ratio equal to zero.

Eq. (28) indicates that H is a function of the damping ratio ξ. Consequently, the identified AO parameters should depend on ξ. Therefore, the sensitivity of the results with respect to the damping ratio has to be addressed. This is the reason why several sets of parameters had been identified for several damping ratios. Table 3 shows that there is almost no influence of the damping ratio on the AO parameters. Moreover, in each case for $\omega = 0$ the apparent mass is equal to the mass of the bar, $m_{\text{st}} = 1726\,\text{g}$, that is the rigid body mode mass. The identified parameters are the same as the ones previously calculated and listed in Table 2.

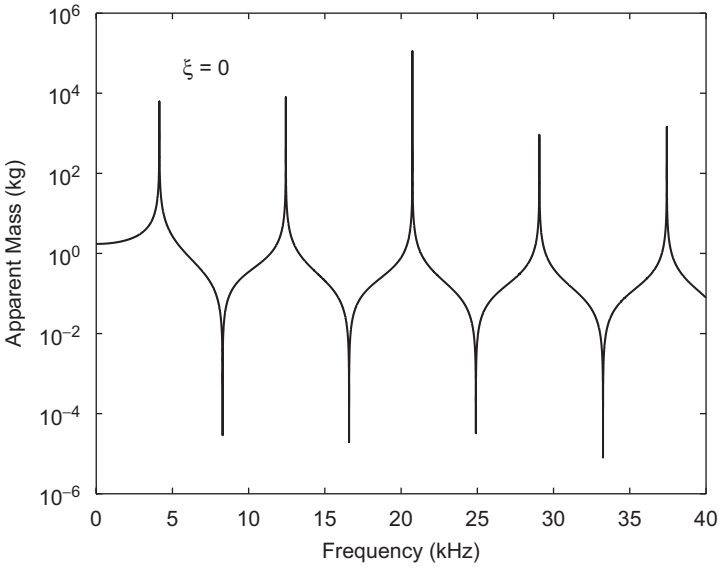

Fig. 3. Free–free bar: apparent mass FRF modulus ($\xi = 0$).

Table 3
Identified AO characteristics for several damping ratios

	$\xi = 0\%$		$\xi = 0.5\%$		$\xi = 5\%$	
	m_i (g)	$f_{\mathrm{AR}\ i}$ (kHz)	m_i (g)	$f_{\mathrm{AR}\ i}$ (kHz)	m_i (g)	$f_{\mathrm{AR}\ i}$ (kHz)
1	1398.8	4.14	1398.4	4.14	1399.6	4.15
2	155.3	12.44	155.2	12.44	155.4	12.44
3	55.5	20.74	55.9	20.74	55.9	20.74
4	28.5	29.07	28.6	29.07	28.5	29.07
5	17.3	37.43	17.3	37.43	17.3	37.43

Table 4
Properties of the beam

E (GPa)	ρ (kg m^{-3})	d (mm)	I (cm^4)	L (mm)
70	2400	20	1.33	1000

Table 5
Characteristics of the AO simply supported beam

AO number	1	2	3	4	5
Mass m_i (g)	251.5	79.0	38.9	23.5	15.8
Frequency f_{AR} (Hz)	310	1040	2289	4207	7028
m_{st} (g)	464.7				
k_0 (kN m^{-1})	44.86				

This example showed that, for a system with a rigid body mode, the numerical point apparent mass FRF was enough to identify the parameters associated with the AO model.

5. Pinned–pinned beam: numerical experiments

In this case, the simply supported beam made of aluminium and of a square cross-section was a determinate structure. The geometry and material characteristics are listed in Table 4.

The procedure is undertaken in the same way as in the previous section where the AO characteristics are determined first from the mass and stiffness matrices and then from the apparent mass FRF.

5.1. Anti-oscillator characteristics from a FE model

The beam was discretized in 20 finite elements. The element used was a Timoshenko beam element, that is with a linear interpolation for the displacement and the rotation, and with two dof per node. The model had 40 dof. The reduced mass and stiffness matrices were then derived from the mass and stiffness matrices. The constraint modes were then obtained by solving the eigenproblem associated with (K^{red}, M^{red}) and finally, the AO characteristics were calculated from Eqs. (22)–(27). The results are given in Table 5.

5.2. Anti-oscillator characteristics from the mass FRF

The FRF were obtained from the eigenmodes of the mass and stiffness matrices, as explained in the previous section. The FRF H given by Eq. (28) is used to determine the static stiffness k_0:

$$H(\omega = 0) = \frac{1}{k_0}. \tag{31}$$

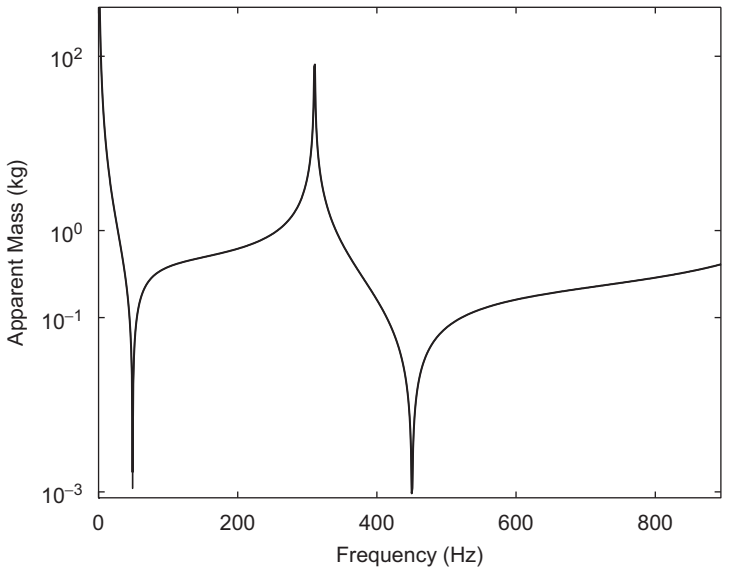

Fig. 4. Simply supported beam: apparent mass FRF modulus ($\xi = 0$).

Similarly, the static mass is derived from the apparent mass FRF, M_{app}:

$$\lim_{\omega \to 0} M_{\text{app}}(\omega) + \frac{k_0}{\omega^2} = m_{\text{st}}. \tag{32}$$

In fact, the actual apparent mass FRF was not suitable to work with due to the asymptote tending to infinity as frequency tends to zero (see Fig. 4). So the modified apparent mass FRF, M^{mod}, defined as following, was more appropriate because the singularity is then removed:

$$M_{\text{app}}^{\text{mod}} = M_{\text{app}} + \frac{k_0}{\omega^2} = m_0 + \sum_{l=1}^{N} \frac{m_i}{1 - (\omega^2/\omega_{\text{AR}\,i}^2)} \tag{33}$$

The modified mass FRF is defined even for ω equal to zero:

$$M_{\text{app}}^{\text{mod}}(\omega) = m_{\text{st}}. \tag{34}$$

This modification increased the accuracy of the N and D polynomial identification. The sensibility of the results with respect to the damping ratio was addressed as well. As observed for the bar in the previous section, it has been verified, that, for this case, there is almost no influence of the damping ratio on the identified parameters.

6. Actual experimental identification of the AO characteristics

The last two examples worked very well, but the data were from numerical simulations and were not influenced by any noise. In this section a pinned–free beam and a pinned–pinned beam are studied. These examples will deal with both determinate and indeterminate structures.

The acceleration was measured with a B&K 4393 accelerometer and a Nexus conditioner while the force was measured with a B&K 8200 transducer force associated with a B&K 2626 conditioner. A Siglab analyser was used to obtain the FRF (the dynamic apparent mass). The sampling frequency was 25.6 kHz.

6.1. Pinned–free (P–F) beam

The studied beam was a cylinder (radius R, length L) made of steel. The pinned support is positionned 19 mm from one end; L is the length if the beam and R is the radius. The geometry and material characteristics

are listed in Table 6. The OA were associated with a measurement point which was 410 mm from the axis of rotation.

The experimental curve is given in Fig. 5: the peaks give the antiresonant frequencies and the zeros give the resonance frequencies. The AO masses were identified as described previously. The AO characteristics are given in Table 7.

Eq. (19) shows that, in that case, the apparent dynamic mass must have a horizontal asymptote when the frequency tends to zero that gives the "static mass" m_{st} (actually m_{st} is a rigid body mass). Indeed experimentally the horizontal asymptote was observed (see Fig. 6) and m_{st} was identified (see Table 7). A direct evaluation of the rigid body mode led to $m_{st} = 186$ g which is closed to the value identified and given in Table 7.

The identified apparent mass FRF was plotted in Fig. 5. The figure shows that the identified AO parameters allowed good reconstruction of the experimental apparent mass FRF.

6.2. Pinned–pinned (P–P) beam

The studied beam was similar to the P–F beam except for the length (see the characteristics listed in Table 8). The OA parameters were associated with a measurement point located at the mid-length. In fact, this beam was not a pure simply supported beam which may be easily seen from the experimental eigenfrequencies. This is essentially due to vertical stiffness induced by the movement of the ball bearing assembly at the ends of the beam (see Fig. 7). Moreover, both bearing assemblies are not fully constrained to avoid the nonlinear effects due to tensile load: the beam can move in a groove made in the bearings.

The experimental curve is given in Fig. 8. The AO masses were identified as described previously. The AO characteristics are given in Table 9.

Table 6
Properties of the P–F beam

E (GPa)	ρ (kg m^{-3})	R (mm)	L (mm)
210	7800	6	500

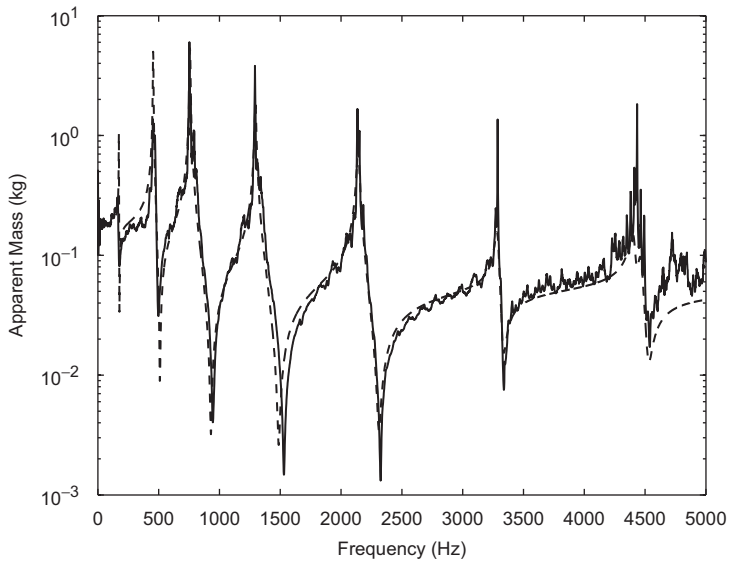

Fig. 5. P–F beam apparent mass FRF modulus: experiment FRF (——) and identified AO FRF (- - -).

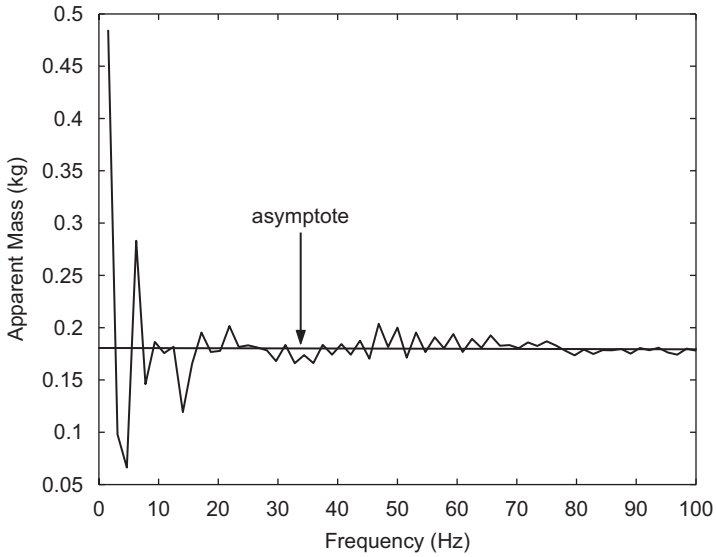

Fig. 6. P–F beam: zoom of the apparent mass FRF (real part).

Table 7
AO characteristics of the P–F beam

AO number	1	2	3	4	5	6	7	8
Mass m_i (g)	15	42.9	44.6	16.8	7.5	1.4	1.1	0.8
Frequency f_{AR} (Hz)	173	455	758	1296	2141	3286	4406	4463
m_{st} (g)	185							
k_0 (kN m^{-1})	0							

Eq. (19) shows that, in that case, the apparent dynamic mass tends to infinity when the frequency tends to zero. This fact was experimentally observed as shown in Fig. 8. This makes the identification more difficult. In Section 5, that was overcome due to the knowledge of the static stiffness k_0. Unfortunately an experimental FRF is not as "perfect" as a numerical FRF, especially in the low frequency domain. In this case, the use of the modified apparent mass FRF was not appropriate. A solution was to multiply Eq. (19) by ω^2 and to obtain the dynamic stiffness FRF:

$$K_{\mathrm{dyn}}(\omega^2) = -k_0 + \omega^2\left(m_0 + \sum_{l=1}^{N} \frac{m_i}{1-(\omega^2/\omega_{\mathrm{AR}\,i}^2)}\right) \tag{35}$$

which had the following asymptote toward zero:

$$K_{\mathrm{asym}}(\omega^2) = -k_0 + \omega^2\left(m_0 + \sum_{l=1}^{N} m_i\right) = -k_0 + \omega^2 m_{\mathrm{st}}. \tag{36}$$

The slope of this asymptote is the static mass, and the absolute value of $K_{\mathrm{asym}}(\omega^2 = 0)$ provides the static stiffness. These parameters have been identified from Fig. 9 and are given in Table 9. By considering the static mode ϕ_{st}, m_{st} may be determined:

$$m_{\mathrm{st}} = \int_0^L \rho S \phi_{\mathrm{st}}^2(x)\,\mathrm{d}x = 17/35 m_{\mathrm{beam}} = 182\,\mathrm{g}, \tag{37}$$

where $\phi_{\mathrm{st}}(x) = -4(x/L)^3 + 3(x/L)$ for $x \in [0, L/2]$ and ϕ_{st} is symmetric with respect to the mid-span section.

Table 8
Properties of the P–P beam

E (GPa)	ρ (kg m^{-3})	R (mm)	L (mm)
210	7800	6	423

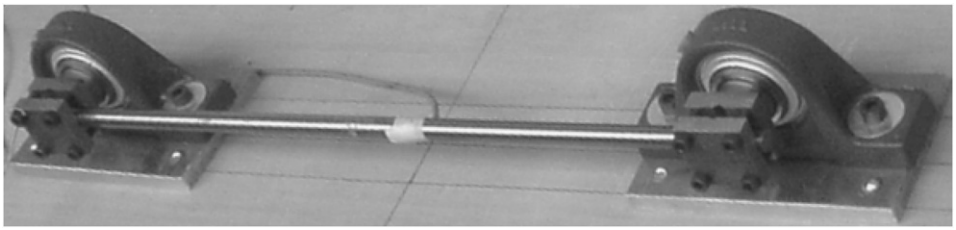

Fig. 7. The pinned–pinned beam.

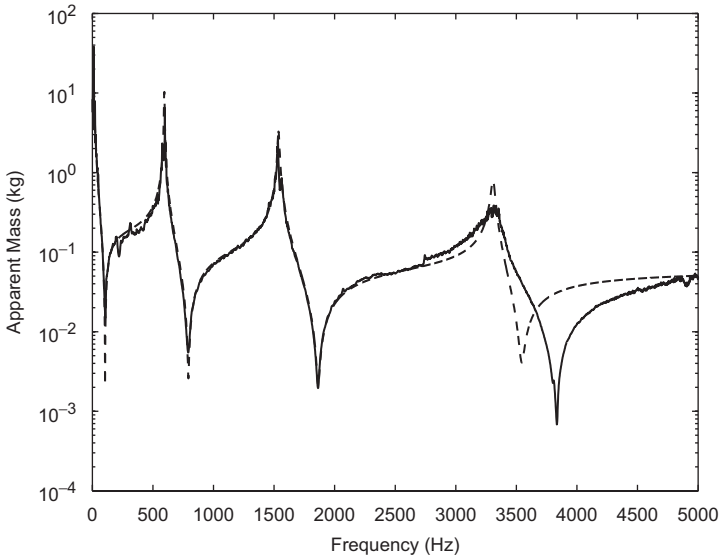

Fig. 8. P–P beam apparent mass FRF modulus: experiment FRF (——) and identified AO FRF (- - -).

Table 9
AO characteristics of the P–P beam

AO number	1	2	3
Mass m_i (g)	8.2	2.92	0.76
Frequency f_{AR} (Hz)	594	1537	3308
m_{st} (g)	180		
k_0 (kN m^{-1})	800		

This proves the accuracy of determining m_{st} with the described method. The static stiffness can also be derived from m_{st} and the first eigenfrequency f_1 ($f_1 = 107$ Hz):

$$k_0 = (2\pi f_1)^2 m_{st} = 813\,\text{kN m}^{-1}. \tag{38}$$

The discrepancy with the value given in Table 9 is around 1%.

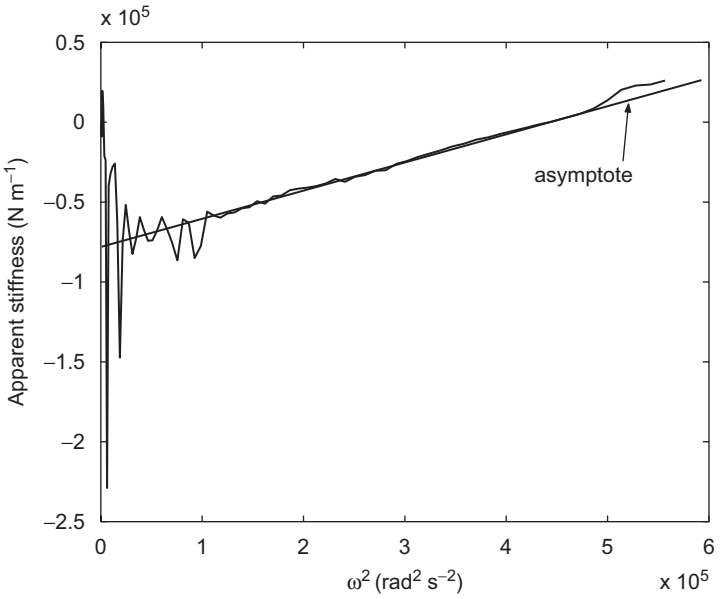

Fig. 9. P–P beam apparent stiffness FRF (real part) and the asymptote (frequency range: [0-120] Hz).

The identified apparent mass FRF was plotted in Fig. 8 which shows that the identified AO parameters allowed good reconstruction of the experimental apparent mass FRF up to 3300 Hz. To decrease the discrepancy beyond 3300 Hz, more AOs are required. They can be identified with the part of the FRF beyond 3300 Hz.

7. Conclusion

The AO model defined in a previous paper [2] was associated to a first model of the studied structure. Accordingly the quality of that model depends on another model. A direct identification of the AO parameters was proposed in this paper to avoid a dependence on a model. This method required the experimental determination of a point apparent mass FRF which may be carried out easily. This point FRF is measured at the location and the direction associated with the required AO. This FRF is a rational function and the first step to get the AO characteristics is to identify that rational function. A partial fraction decomposition of the point apparent mass FRF is then achieved. The residues of the decomposition are the AO masses and the poles are the antiresonant frequencies.

The only difficulties arose to identify the static stiffness and the static mass. For indeterminate structure, the static mass is the y-intercept of the FRF curve and it may be obtained by drawing the asymptote of the FRF when the frequency tends to zero. For determinate structure the apparent mass FRF has a singularity at zero. So, a solution to identify the static stiffness and the static mass is to use the dynamic stiffness FRF which has an asymptote when the frequency tends to zero. The slope of this line is the static mass while the static stiffness is the y-intercept.

Consequently, this paper shows that it is possible to build easily a model of a structure with a basic experiment. Moreover, the parameters of this model give some a priori information on the impact behaviour of the structure as indicated in Ref. [8]. So the AO model is useful not only to simulate the response of a structure but also to understand how a structure behaves when impacted.

As the AO parameters may be experimentally and numerically obtained, it is then possible to have a new indicator of the accuracy of a model by comparing the AO parameters of both models. This may be explored in the future by researchers interested in updating structures.

References

[1] T.J.R. Hughes, *The Finite Element Method*, Dover Publication, 2000.
[2] E. Jacquelin, J.P. Lainé, A. Bennani, M. Massenzio, A modelling of an impacted structure based on constraint modes, *Journal of Sound and Vibration* 301 (3–5) (2007) 789–802.
[3] F. Wahl, G. Schmidt, L. Forrai, On the significance of antiresonance frequencies in experimental structural analysis, *Journal of Sound and Vibration* 219 (3) (1999) 379–394.
[4] D.A. Rade, G. Lallement, A strategy for the enrichment of experimental data as applied to an inverse eigensensitivity-based FE model updating method, *Mechanical Systems and Signal Processing* 12 (2) (1998) 293–307.
[5] J.E. Mottershead, On the zeros of structural frequency response functions and their sensitivities, *Mechanical Systems and Signal Processing* 12 (5) (1998) 591–597.
[6] W. D'Ambrosio, A. Fregolent, The use of antiresonances for robust model updating, *Journal of Sound and Vibration* 219 (3) (1999) 379–394.
[7] M. Dilena, A. Morassi, The use of antiresonances for crack detection in beams, *Journal of Sound and Vibration* 276 (2004) 195–214.
[8] S. Pashah, M. Massenzio, E. Jacquelin, Structural response of impacted structure described through anti-oscillators. *International Journal of Impact Engineering* (2007), doi:10.1016/j.ijimpeng.2007.06.004.
[9] D.J. Ewins, *Modal Testing*, Research Studies Press Ltd., 2000.